Annals of Operations Research (2025) 344:499–531
https://doi.org/10.1007/s10479-024-06287-9

ORIGINAL - OR MODELING/CASE STUDY

Optimizing the economic dispatch of weakly-connected mini-grids under uncertainty using joint chance constraints

Nesrine Ouanes[1] · Tatiana González Grandón[2] · Holger Heitsch[3] · René Henrion[3]

Received: 28 February 2024 / Accepted: 10 September 2024 / Published online: 25 September 2024

Abstract
In this paper, we deal with a renewable-powered mini-grid, connected to an unreliable main grid, in a Joint Chance Constrained (JCC) programming setting. In several rural areas in Africa with low energy access rates, grid-connected mini-grid system operators contend with four different types of uncertainties: forecasting errors of solar power and load; frequency and outages duration from the main-grid. These uncertainties pose new challenges to the classical power system's operation tasks. Three alternatives to the JCC problem are presented. In particular, we present an Individual Chance Constraint (ICC), Expected-Value Model (EVM) and a so called regular model that ignores outages and forecasting uncertainties. The JCC model has the capability to guarantee a high probability of meeting the local demand throughout an outage event by keeping appropriate reserves for Diesel generation and battery discharge. In contrast, the easier to handle ICC model guarantees such probability only individually for different time steps, resulting in a much less robust dispatch. The even simpler EVM focuses solely on average values of random variables. We illustrate the four models through a comparison of outcomes attained from a real mini-grid in Lake Victoria, Tanzania. The results show the dispatch modifications for battery and Diesel reserve planning, with the JCC model providing the most robust results, albeit with a small increase in costs.

Keywords Joint chance constraints · Mini-grid operation · Unreliable main grid · Stochastic forecasting errors · Spherical radial decomposition

✉ Nesrine Ouanes
nesrine.ouanes@hu-berlin.de

Tatiana González Grandón
tatiana.c.g.grandon@ntnu.no

Holger Heitsch
heitsch@wias-berlin.de

René Henrion
henrion@wias-berlin.de

[1] Chair for Management Science, Humboldt University Berlin, Spandauer Straße 1, 10178 Berlin, Germany

[2] Department of Industrial Economics and Technology Management, Norwegian University of Science and Technology, Sentralbygg 1, Gløshaugen Trondheim, Norway

[3] Weierstrass Institute Berlin, Mohrenstraße 39, 10117 Berlin, Germany

Index

$t \in T$	Set of time steps
τ	Subset of time-steps when outages could start

Parameters

T	Total number of time steps
$c_{\Lambda,t}$	Marginal cost of Diesel at time t [$/kWh]
$c_{b,t}$	Marginal aging cost of battery at time t [$/kWh]
$c_{g,t}$	Cost of day-ahead grid import at time t [$/kWh]
$p_{g,t}$	Price for day-ahead grid export at time t [$/kWh]
$c_{\gamma,t}$	Cost function for instantaneous grid exchange [$]
$p_{d,t}$	Price for electricity sales at time t [$/kWh]
η^+	Average efficiency of battery charge [%]
η^-	Average efficiency of battery discharge [%]
σ	Average battery self-discharge rate (internal resistance) [%]
κ	Average duration of outages [h]
$\Lambda^{\max}$	Rated capacity of diesel [kW]
$b^{\max}$	Maximum charging / discharging rate [kW]
$SOC^{\max}$	Maximum state of charge of the battery [kWh]
$SOC^{\min}$	Minimum state of charge of the battery [kWh]
SOC_0	Initial state of charge of the battery [kWh]
s_t	Forecasting of solar production at time t [kW]
g^{max}	Maximum available grid capacity at time t [kW]
d_t	Load forecasting at time t [kW]
p	Probability of successful islanding [-]
ω	Probability of an outage happening during one optimization horizon [-]

Random variables

δ_t	Load forecasting error at time t [kW]
ξ_t	Forecasting error of solar power at time t [kW]
γ_t	Slack grid exchange at time t [kW]

Non-negative decision variables

Λ_t	Diesel power at t [kW]
g_t^+	Electricity imported from the main grid at time t [kW]
g_t^-	Electricity exported to the main grid at t [kW]
b_t^+	Battery charge at time t [kW]
b_t^-	Battery discharge at time t [kW]
SOC_t	State of charge at time t [kWh]
r_t^b	Reserve for the battery discharge at time t [kW]
r_t^Λ	Reserve for the diesel at time t [kW]

1 Introduction

The United Nations' Sustainable Development Goal 7 (SDG-7) urgently calls for universal access to clean energy, a mission that faces challenges despite increased electrification efforts. Projections by the international energy agency estimate that by 2030, around 650 million people might still lack access, and 9 out of 10 will be in West, Central, and East Africa

(IEA, 2020). Electrification via centralized grids is slow and expensive, prompting interest in decentralized mini-grid energy systems that offer quicker deployment and enhanced cost competitiveness (Antonanzas-Torres et al., 2021).

Renewable-powered mini-grids (MGs) as defined by González Grandón et al. (2021) and Inensus (2014) are hybrid electricity supply systems combining wind turbine or photovoltaic (PV) generation (from 10 kW to 10 MW), energy storage systems, and (usually) a Diesel generator into low and medium voltage distribution networks. Classified by their relationship with the main power grid, MGs come in two forms: islanded mini-grids which operate independently, detached from the national (main) network and grid-connected mini-grids which link with the main grid and function as both backup systems for distribution as well as standalone units.

This article focuses on the operational intricacies of grid-connected mini-grids, situated within the urban and peri-urban areas of Sub-Saharan African countries lacking in energy access. The paradox lies in the fact that, despite the presence of central-grid infrastructure, an alarming number of households, numbering in the hundreds of millions, still grapple with the challenge of accessing less than four hours of electricity per day (Rocky Mountain Institute, 2018). To counter this issue, governments in these countries are progressively adopting grid-connected mini-grids in areas with unreliable main grid supply. Yet, technical uncertainties inherent to grid-connected mini-grids in this context stem from multiple sources: stochastic solar power and demand forecast errors; absolute uncertain main grid outage onset times; and outage durations subjected to statistical analysis. As operational decisions are taken prior to the observation of the uncertainty, it becomes imperative to adopt suitable modeling methodologies that can effectively incorporate all these diverse forms of uncertainty. Thus, our primary research aim focuses on addressing the four mentioned uncertainties through modeling and algorithmic approaches, utilizing Joint Chance Constraints. Additionally, the study aims to assess the effectiveness of the proposed scheduling strategy by applying it to a case study example of a mini-grid in Lake Victoria.

Introduced by Charnes and Cooper (1959), chance constraints offer an appealing tool for dealing with uncertainty in the constraints of an optimization problem. A classical and fundamental introduction to the theory and numerical treatment of chance constraints is presented by Prékopa (1995). A modern treatment is provided by Shapiro et al. (2014). Since their introduction, chance constraints have become common for economic dispatch problems, notably in hydro reservoir management (e.g., Berthold et al., 2022; Loiaciga, 1988; Prékopa & Szántai, 1978; van Ackooij et al., 2014), but also in power dispatch (e.g., Hong et al., 2022; Peña-Ordieres et al., 2021). For mini-grid or micro-grid dispatch, the approach has predominantly involved the use of purely-deterministic predictive models (González Grandón et al., 2021; Parisio et al., 2014). There is increasing interest, however, in applying probabilistic models in order to ensure sufficiently safe satisfaction of demand in a highly stochastic environment, not only with respect to renewable energy but also with respect to instabilities of the main grid. Zhao et al. (2014) and Liu et al. (2017) introduce the interesting concepts of *probability of self-sufficiency* and *probability of successful islanding*, respectively, in order to model the self-sufficiency of a mini-grid when isolated from the main grid by an outage. These concepts rely on keeping reserves for Diesel employment and battery discharge such that an outage of the main grid, to which the mini-grid is connected, can be survived based on these reserves with sufficiently high probability. The shortcoming of the models by Zhao et al. (2014) and Liu et al. (2017) is that they use individual (separate for each time in the given interval) chance constraints. While such a model is comfortable to handle since the chance constraint can be transformed without effort into an explicit equivalent, it does not really reflect the wish for robust self-sufficiency. Indeed, even if one may guarantee that

self-sufficiency holds true at each time individually with high probability, the probability of violating self-sufficiency at **some** time may be high as well (or: the probability of guaranteeing self-sufficiency throughout a given period of time may be small). This is why we will rather consider **joint** chance constraints in this paper which are, however, more difficult to deal with. Indeed, they require the consideration of probabilities and their sensitivities with respect to the decision vector under multivariate random distributions. For numerical solutions related with joint chance constraints, we shall make use of the so-called *spherical-radial decomposition* of Gaussian random vectors which efficiently applies to Gaussian, Gaussian-like (e.g. multivariate log-normal, Gaussian mixture) or elliptically symmetric (e.g. multivariate Student) distributions and has found a lot of applications both in operations research and optimal control under PDEs with random coefficients (e.g., Berthold et al., 2022; Farshbaf-Shaker et al., 2020; González Grandón et al., 2017; Heitsch, 2020). The possibly striking difference between individual and joint chance constraints has been widely studied (e.g., Van Ackooij et al., 2010, p. 547); (Berthold et al., 2022, p. 34).

In this paper we focus on the challenges arising from the model with joint chance constraints. Therefore, we keep some other modeling aspects simple. In particular, we will not include binary decisions (simplified model for Diesel generator), we will not adequately model realistic battery ageing by means of differential equations and we will keep all decisions to be static with respect to the unfolding of uncertainty over time (thus ignoring the gain of information based on random observations prior to decision taking). The inclusion of all these aspects is subject of current and future work, e.g., by González Grandón et al. (2022).

This article makes two key contributions, namely to the realm of applied joint chance constraint programming and to the advancement of SDG-7. More precisely, our analysis involves the following steps:

- We base our input data on real power measurement data obtained from an operating MG in Tanzania and use forecasts for their solar PV generation and the electricity demand of the connected households.
- We propose a model for an economic scheduling strategy of a MG connected to a weak main grid with a specified high reliability level. This model utilizes joint chance constraints, taking into account various uncertainties, including: 1) forecasting errors in renewable power generation, 2) forecasting errors in demand profiles, and uncertainties related to 3) frequency and 4) duration of outages.
- We compare the proposed JCC model with three alternatives. We contrast results with an Individual Chance Constraint, Expected-Value Model and a (mainstream) so-called regular model that ignores outages and forecasting errors.

2 Mini-grid topology and modelling assumptions

Figure 1 illustrates the grid-connected mini-grid configuration. This arrangement includes a solar PV generation unit, one battery energy-storage system (BESS), one Diesel genset, and one connection to an unreliable main-grid.

The PV and BESS are integrated into the system via two distinct inverters linked to the Alternating Current (AC) bus. Interactions with the main grid occurs at the Point of Common Coupling (PCC). At the PCC, a transformer modifies the voltages, translating them from the lower level of the mini-grid to the higher-level of the primary grid (referred to hereafter as main grid or higher-level grid). In the examined context of this paper, this connection to

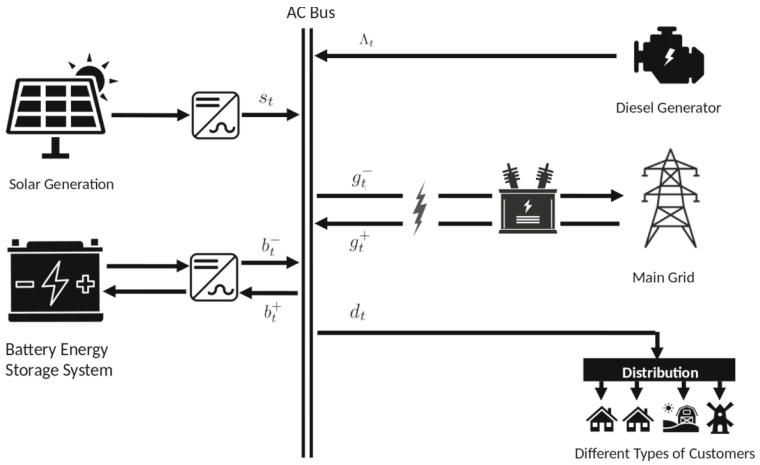

Fig. 1 Weakly Grid-connected Mini-grid Topology

the main grid is unreliable, with outages occurring frequently due to failures in the main grid. This could be an overloading of the main grid, an uncurtailed excess generation or technical aspects due to failures of control strategies, physical components or transmission lines overheating. Lastly, the Diesel genset, acting as a supplementary component to bridge any electricity supply gaps, generates AC current directly, injecting it into the AC bus.

Since the MG is balanced through an AC bus, both active and reactive powers will flow to the loads. In this paper, for simplicity purposes, we assume that the loads of all connected households maintain a purely resistive nature. We, therefore, conduct all our modelling using only active power flow figures, neglecting all reactive components.

Further on, we neglect any temperature effects on the MG components and operation, especially for the battery storage system. The latter is modelled as one large synchronized unit that can either be charged or discharged, thus neglecting specific dynamics between the battery packs. Additionally, we model charging and discharging losses in the battery inverter as well as the battery's internal resistance as single, average efficiency parameters.

In terms of the flexibility of dispatch, we assume that the Diesel genset is able to run between 0 and a maximal capacity, without any ramping constraints or restrictions on minimal resting and running times. Moreover, we follow the premise that the MG operator always maintains a continuous fuel supply. Additionally, we assume that the solar PV output can be controlled with the help of a Charge Controller (CC). In case of an excess of PV generation and an outage preventing any export to the main grid, the PV output can be curtailed fast enough such that the overall local power balance can be withheld.

To model the demand-side, we aggregate all electricity loads into one node, thus neglecting any line losses that occur at the local distribution level. Finally, we assume that the MG operator has access to time series forecasting of solar power generation and aggregate demand for the forthcoming 24 or 48-hour time interval. Furthermore, we assume that, when an outage of the main grid occurs, the power exchange at the PCC drops to 0, thus preventing any planned imports or exports. Outages can occur with a given probability at any arbitrary moment, the precise timing of which remains uncertain. We further assume that there is statistical evidence about the average duration of an outage from the main-grid (Klugman et al., 2021). Table 1

Table 1 Mini-grid uncertainties

Source of uncertainty	Assumptions
Aggregate demand	Access to a forecasting time series for the forthcoming 48 h
Solar PV generation	Access to a forecasting time series for the forthcoming 48 h
Timing of main grid outages	Unknown
Duration of main grid outages	Access to statistical evidence as an exogenous parameter (Klugman et al., 2021)

summarizes the uncertainties present at the examined MG and assumptions made about their modeling.

3 Mathematical models

This section defines the mathematical model used for the above described MG topology. As mentioned before, our aim is to find the optimal dispatch of a weakly-connected MG which allows one to survive a failure of the main grid by means of local energy supply (battery, Diesel). In order to achieve this goal, in addition to the planning of a regular dispatch for strongly connected MGs, reserves for Diesel and battery are included into the model. These can then be employed in the islanded mode of the MG in order to meet the local power demand. Since dispatch has to be planned prior to observing randomness in demand, solar radiation and outages, methods of stochastic optimization come into play. Inspired by the work of Zhao et al. (2014) and Liu et al. (2017), we find the application of probabilistic or chance constraints to be most appropriate here. They provide the possibility to find an optimal dispatch including reserves for Diesel and batteries such that the local demand in an islanded mode caused by an outage is met with a given probability (typically close to one). However, as mentioned in the introduction, these papers handle probability individually in time. While this approach eases drastically the computational treatment of chance constraints, it does not guarantee robust demand satisfaction **throughout** the whole critical time interval. Therefore, our main contribution is devoted to model the MG dispatch problem with respect to joint chance constraints. This type of constraints cannot directly be converted into explicit linear constraints as in the individual case, but requires to deal with probability functions and their derivatives under multivariate distributions.

This section is organized as follows: after introducing the used nomenclature, we present the objective function and the (common) deterministic constraints for the optimization problem. Then, we introduce our additional joint chance constraints with respect to decisions on keeping reserves. We shall assume that an outage may occur at most once a day with a given probability. Its initial time is supposed to be uniformly distributed over the day. As for the duration of the outage, we either fix it (e.g., as a statistical mean from available historical data) or consider it to be an exterior parameter which can be varied in different computations. Next, we move on to a model with individual chance constraints as used by Zhao et al. (2014) and Liu et al. (2017), in order to illustrate the gain in robustness by using joint chance constraints. Finally, for the sake of completeness, we also mention two further simplifications of the model: first, the *expected-value model* in which we replace all random parameters by

their expected values, such that statistical information is reduced to the first moment. Second, the widely-used *regular model*, which in addition to the previous simplification, also completely ignores the possibility of outages (Beath et al., 2023; Elegeonye et al., 2023; González Grandón et al., 2021; Kumar, 2021; Kumar and Pahuja, 2021).

3.1 Objective functions

In this subsection, we will introduce the objective function used across the mathematical models starting with the cases of a strongly-connected and a weakly-connected mini-grid.

Strongly-connected mini-grid

We first present the objective function for a strongly-connected mini-grid, i.e., where outages do not occur. In such a mini-grid, if the operator faces forecasting errors in solar and load predictions, the impact is negligible from a physical standpoint. The system can be adapted by managing exports and imports. However, economically, it's important to note that instantaneous grid exchanges come with a higher cost compared to day-ahead exchanges.

For such a problem, we want to maximize the profit of the MG dispatch, which is equivalent to minimizing the net operational costs minus net revenue. The summation term in the objective (1) reflects the negative profit of the MG over the nominal time horizon T, plus the duration of an outage κ, as the outage could start at the end of the nominal time horizon.

$$f_0(\Lambda, b^+, b^-, g^+, g^-) := \sum_{t=1}^{T+\kappa} c_{\Lambda,t} \cdot \Lambda_t + c_{b,t} \cdot (b_t^+ + b_t^-) - p_{d,t} \cdot d_t + c_{g,t} g_t^+ - p_{g,t} g_t^- + \mathbb{E}[c_{\gamma,t}(\gamma_t)]. \quad (1)$$

The aim is to maximize the profit of the MG dispatch, i.e., minimize the function f_0, where revenues from electricity sales are subtracted from the marginal costs of operation. The marginal costs consist of the fuel costs $c_{\Lambda,t}$ for the Diesel genset, of the battery lifetime depreciation costs $c_{b,t}$ due to the discharge-charge cycling, and of the costs $c_{g,t}$ for importing from the main grid. Solar power is assumed to have zero marginal costs and therefore doesn't appear in the objective function. Thus far, maintenance costs are not explicitly considered. They could be levelized and included in the cost coefficients of each technology. However, for this paper, further considerations about the maintenance approach are omitted. The revenues are generated from selling the electricity at exogenous price of $p_{d,t}$ to the connected households consuming electricity at the MG level, as well as from exporting excess electricity at the exogenous price of $p_{g,t}$ to the main grid. The random variable

$$\gamma_t = \gamma_t(z, \xi, \delta) := d_t + \delta_t - s_t - \xi_t - \Lambda_t - b_t^- + b_t^+ - g_t^+ + g_t^-, \ \forall t = 1, \ldots, T + \kappa, \quad \text{with } z := (\Lambda, b^-, b^+, g^-, g^+), \quad (2)$$

is defined as the compensating action establishing the load balance after applying the decisions z on the employment of Diesel Λ_t, battery b_t and grid exchange g_t on a day-ahead approach and observing the random variables solar energy $s_t + \xi_t$ and demand $d_t + \delta_t$ (given forecast plus random deviation in both cases). A positive value of γ_t represents a lack of energy to be compensated by instantaneous import from the main grid (at a price that may be substantially higher than for the import on the day ahead market). A negative value of γ_t refers to an excess of energy which has to be instantaneously exported to the grid, again at certain costs (so that,

contrary to the day ahead market there is no reward for the export). As γ_t and, hence, its associated costs, are random, we minimize the expectation of these costs.

All costs and prices are defined as time-variable parameters, hence the index t for each of these parameters.

Weakly-connected mini-grid

Here, we introduce the intricacies associated with a weakly-connected MG, i.e. with potential outages in the main grid and adjust the objective function accordingly. Starting with the initial objective function (1), we adapt the objective function f_0 to account for the case of possible grid outages. We introduce the following definition:

$$
\begin{aligned}
&f_1(\Lambda, b^+, b^-, g^+, g^-, r^\Lambda, r^b) := \\
&\sum_{t=1}^{T+\kappa} c_{\Lambda,t} \cdot \Lambda_t + c_{b,t} \cdot (b_t^+ + b_t^-) - p_{d,t} \cdot d_t \\
+\frac{\omega}{T} \sum_{\tau=1}^{T} &\left(\sum_{t=1, t\neq\tau,\ldots\tau+\kappa}^{T+\kappa} c_{g,t} g_t^+ - p_{g,t} g_t^- + \mathbb{E}[c_{\gamma,t}(\gamma_t(z,\xi,\delta))] + \sum_{t=\tau}^{\tau+\kappa} c_{\Lambda,t} r_t^\Lambda + c_{b,t} r_t^{b-} \right) \\
&+(1-\omega) \sum_{t=1}^{T+\kappa} \left(c_{g,t} g_t^+ - p_{g,t} g_t^- + \mathbb{E}[c_{\gamma,t}(\gamma_t(z,\xi,\delta))] \right). \qquad (3)
\end{aligned}
$$

The first term is defined in analogy to (1) including again a summation over the Diesel and battery cycling costs minus the revenues generated by selling the electricity to local customers at a given price. Now, considering the possibility of grid outages, we delineate two scenarios for the costs and revenues associated with grid exchange: one when an outage occurs and another when it does not. These scenarios are articulated in the second and third terms of (3). We make the assumption that, at most, one outage may occur during the designated day ahead, and the probability of its occurrence is denoted as ω. In the absence of an outage during the specified day (probability equals $1-\omega$), the sole additional costs stem from trading with the main grid (third term). Conversely, when an outage occurs, suppose at time τ, then in the interval $[\tau, \ldots, \tau+\kappa]$, representing the duration of the outage, no trading costs with the main grid are incurred (due to the lost connection). However, additional costs arise from utilizing reserve capacities r_t^Λ, r_t^{b-} for Diesel generation and battery discharge to meet the local demand in the islanded mode (second term).

We assume that τ is uniformly distributed, indicating that an outage may initiate at any time with equal probability. Consequently, in the second term of (3), we compute the average costs across all potential starting times for the outage. In contrast, the duration κ of the outage is regarded as the statistical mean derived from historical data or treated as an exogenous parameter of the problem, capable of assuming multiple values.

3.2 Deterministic constraints

The physical constraints represent well-known formulations for mini-grid economic dispatch models, consisting in capacity constraints of the MG components, a power balancing constraint for MG supply and demand, inter-temporal constraints for the storage state of charge, as well as considerations of conversion and distribution losses expressed through average efficiency parameters. These will be discussed in more detail in the following.

Capacity constraints of the Diesel genset: it is assumed that the Diesel genset can operate between 0 and its maximal capacity Λ^{max}. Therefore, the sum of the decision variables for

the Diesel genset dispatch Λ_t and the Diesel genset reserve r_t^{Λ} have to be within these bounds at all time (4).

$$0 \leq \Lambda_t + r_t^{\Lambda} \leq \Lambda^{max}, \qquad \forall t = 1, \ldots, T + \kappa. \tag{4}$$

Capacity constraints of the battery charge and discharge: similarly to the Diesel genset, the battery charge and discharge rates are also bound by a lower level of 0 and an upper level b^{max}. In the case of discharging the battery, we define the discharge rate as the sum of the actual dispatch decision b_t^- and the planned reserve r_t^b (5). Since we assume that the reserves are used to compensate an electricity shortage and that any excess generation from solar PV can be curtailed fast enough, we omit the definition of a reserve for the battery charging, thus obtaining the constraint (6) for the decision variable of battery charging b_t^+.

$$0 \leq b_t^- + r_t^b \leq b^{max}, \qquad \forall t = 1, \ldots, T + \kappa. \tag{5}$$

$$0 \leq b_t^+ \leq b^{max}, \qquad \forall t = 1, \ldots, T + \kappa. \tag{6}$$

Capacity constraint for the grid exchange: the connection to the main grid at the PCC is also constrained by a certain capacity limit over time. Thus, the decision variables for the grid export g_t^- and the grid import g_t^+ are also bound by an upper value of g_t^{max}:

$$0 \leq g_t^+ \leq g_t^{max}, \qquad \forall t = 1, \ldots, T + \kappa. \tag{7}$$

$$0 \leq g_t^- \leq g_t^{max}, \qquad \forall t = 1, \ldots, T + \kappa. \tag{8}$$

Power balancing constraint: as in any power system, to maintain the system frequency and prevent any voltage surge or sag that would lead to a grid failure, the supply and demand of electricity must be equal at any time. As mentioned in Sect. 3.1, this balance is established by means of the compensating action γ_t defined in (2), where any current excess or deficit in the load balance is rectified by instantaneous (potentially costly) grid exchange

$$s_t + \xi_t + \Lambda_t + b_t^- - b_t^+ + g_t^+ - g_t^- + \gamma_t = d_t + \delta_t \quad \forall t = 1, \ldots, T + \kappa. \tag{9}$$

Capacity, cycling and inter-temporal constraints for the battery energy-storage system: in addition to the constraints on the battery discharge and charge rates defined in constraints (5) and (6), we need to define additional constraints on the battery energy fill level, also called State Of Charge (SOC), and defined in the following constraints as SOC_t. The first constraint concerns the upper and lower bounds of the SOC which are defined by both physical constraints of the actual battery size, as well battery protection measures that set tighter conditions on these bounds (SOC^{min} and SOC^{max} in the constraint (10)) in order to protect the battery from overheating and extend its lifetime.

$$SOC^{min} \leq SOC_t \leq SOC^{max}, \qquad \forall t = 1, \ldots, T + \kappa. \tag{10}$$

In the second constraint for the battery energy-storage system, we set a condition to the cycling of the battery over the nominal time horizon T, which guarantees that battery's SOC at the the end of each time horizon T is equal to the SOC at the beginning of the time horizon as defined in the constraint (11). With this, we make sure that the dispatch is optimized with the ulterior operation of the MG, beyond the nominal time horizon, is considered and the SOC at the end of the time horizon is not exhausted for subsequent operational time steps. This constraint is optional, since, in practice, the optimization of the MG operation is usually conducted in a rolling horizon approach, preventing such exhaustion of the SOC at the end of an optimization horizon.

$$SOC_T = SOC_0. \tag{11}$$

In the next constraint for the battery energy-storage system, we look into the inter-temporality of the battery discharge and charge processes, which translates into an increase or a decrease of the SOC over time. For this, we define the constraint (12), which relates the SOC at time t to the SOC at time $t-1$, with the initial value SOC_0 given. The relation between SOC_t and SOC_{t-1} takes into account the battery discharge b_t^- and charge b_t^+ multiplied by their respective average efficiency coefficients η^+ and η^-. Since b_t^- and b_t^+ are power figures, expressed in kW or W and the SOC is an energy figure expressed in kWh or Wh, the net charge and discharge rate must be multiplied with the nominal time-step Δt,

$$SOC_t = SOC_{t-1} + (\eta^+ b_t^+ - \eta^- b_t^-)\Delta t, \qquad \forall t = 1, \ldots, T + \kappa. \tag{12}$$

Finally, we define the constraint (13) to describe the potential discharge of the battery, and therefore the potential SOC, in case of an employment of the battery reserves because of an outage. This potential SOC at time t (SOC_t) minus the cumulative reserves r_s^b that are planned in the κ previous time steps, multiplied by the average discharging efficiency η^- and the nominal time-step Δs. Since r_s^b is a non-negative decision variable, the constraint (13) entails the definition of the lower bound presented in the constraint (10).
For $t = 1, \ldots, T + \kappa$:

$$SOC^{min} \leq SOC_t - \sum_{s=\tau}^{\min\{\tau+\kappa, t\}} \eta^- r_s^b \Delta s, \quad \tau = 1, \ldots, \max\{t - \kappa,\ 1\}. \tag{13}$$

Since we consider a battery reserve only for the discharging, we do not need to define an adjusted constraint for the upper bound of the potential SOC. Therefore, the definition of the upper bound in the constraint (10) remains unchanged.

3.3 Random parameters

In this section, we describe how the random parameters, namely solar energy and demand are dealt with in our model.

Time series analysis

Apart from the fixed data, two data sets are used in this study: solar data in dry season and rural load data. In this study, we implement an Autoregressive Integrated Moving Average (ARIMA) model (Box and Jenkins, 1976) to forecast the next 48 h (such that we can vary κ to explore different scenarios). ARIMA models have a single dependent variable that is a linear function of past values and an error term. Integrated processes are typically non-stationary. There are two main sources of non-stationarity: (a) heteroscedasticity, which can often be addressed by applying a log transformation; (b) an increasing or decreasing trend, which can often be eliminated by differencing. Differencing the series d times yields a stationary stochastic process. A typical ARIMA(p, d, q) model can be expressed by:

$$\varphi_p(B)(1 - B)^d z_t = \theta_q(B)\varepsilon_t \tag{14}$$

where z_t represents a non-stationary time series at time t, ε_t is a white noise, d is the order of differencing, B is the backward shift operator defined by $Bz_t = z_{t-1}$ and $\varphi_p(B)$ is the autoregressive operator defined as:

$$\varphi_p(B) = 1 - \varphi_1 B - \varphi_2 B^2 - \cdots - \varphi_p B^p. \tag{15}$$

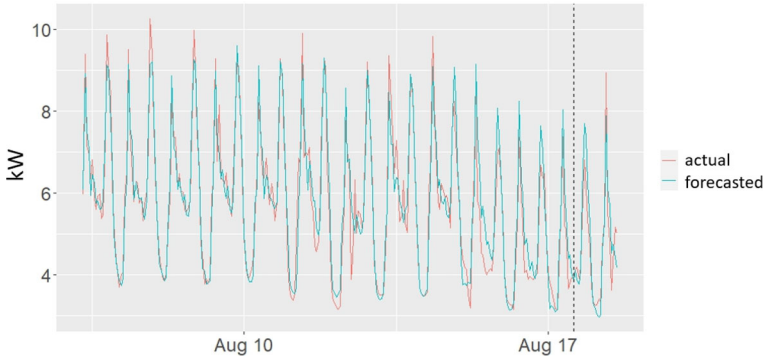

Fig. 2 Actual and forecasted ARIMA(24, 1, 27) load model

Also, $\theta_q(B)$ is the moving average operator defined as:

$$\theta_q(B) = 1 - \theta_1 B - \theta_2 B^2 - \cdots - \theta_q B^q \tag{16}$$

To determine appropriate parameters of the ARIMA models, the following method used in Sen et al. (2016); González Grandón et al. (2024) was applied. Firstly, the lowest order of differencing needed for the series to become stationary was identified. This is done by utilizing the *auto.arima* function within the *R forecast* package (R Core Team, 2021). Based on the high p-value of the differenced time series from the Kwiatkowski-Phillips-Schmidt-Shin (KPSS), we confirm stationarity. The differenced stationary time-series is then tested with an autocorrelation function (ACF) and partial autocorrelation function (PACF) to determine the highest orders of p and q respectively for which significant auto-correlation is left. The obtained values are then used as an upper limit for a step-wise grid search with varying p and q values starting from 1 respectively. The d value determined by the *auto.arima* function is retained fixed. ARIMA models are then computed for all specified combinations of (p, d, q) values and we select the one with the lowest Akaike Information Criterion (AIC). Initial estimates for the AR and MA coefficients are obtained using conditional-sum-of-squares estimation, followed by maximum likelihood estimation to finalize these coefficients. Lastly, the model performance was evaluated using Root Mean Square Errors (RMSEs) and coefficient of determination R^2.

For the rural load data the best model we obtain is an ARIMA(24,1,27). The comparison between the actual value and the forecasting value for the 48 points out-of-sample is given in Fig. 2.

Similarly, the best model we got for the solar power production during the dry season was an ARIMA(12,0,13) and the forecasted values for a 48 h test set are shown in Fig. 3.

We conducted a comprehensive statistical residual analysis on the ARIMA models to evaluate the appropriateness of the model fit. Our investigation revealed that the residuals from rural load, denoted as δ_t, from solar forecasts, denoted as ξ_t, conform to a normal distribution with zero mean. The Shapiro test resulted in a p-value of 3.2×10^{-3} for load and of 6.4×10^{-5} for solar.

Furthermore, we assumed that the forecasting error of rural load δ is independent from the forecasting error of solar power ξ. This assumption and the aforementioned time series

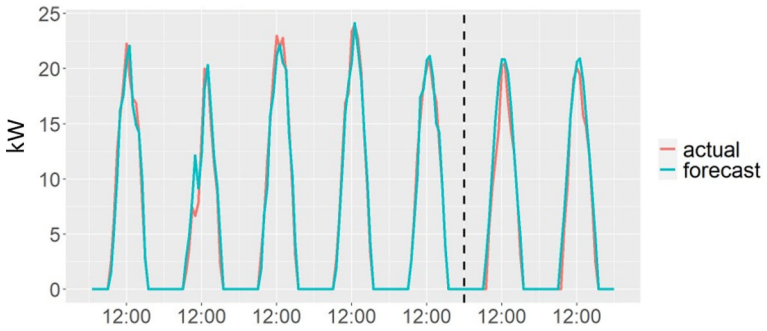

Fig. 3 Actual and forecasted ARIMA(12, 0, 13) solar power model

analysis imply that:

$$X := \begin{pmatrix} \xi \\ \delta \end{pmatrix} \sim \mathcal{N}\Big(\begin{pmatrix} \mu_\xi \\ \mu_\delta \end{pmatrix}, \tilde{\Sigma} \Big) \quad \text{, where } \tilde{\Sigma} = \begin{pmatrix} \Sigma_{\xi\xi} & 0 \\ 0 & \Sigma_{\delta\delta} \end{pmatrix}. \tag{17}$$

As will be derived later for the definition of the joint and individual chance constraints (in (22) and (21) respectively), the random vectors ξ and δ are incorporated into the constraints as a net vector $\alpha := \delta - \xi$, characterized by a non-degenerate Gaussian distribution. With the assumption of independence, which implies zero correlation, and considering the zero mean result explained above, (17) is simplified to obtain:

$$\begin{aligned} \mu_\alpha &= \mu_\delta - \mu_\xi = 0, \\ \Sigma_\alpha &= \Sigma_{\xi\xi} + \Sigma_{\delta\delta}. \end{aligned} \tag{18}$$

The non-degenerate Gaussian nature of the distribution of α holds particular significance as one of the crucial theoretical and numerical aspects concerning our joint chance constraint problem which pertains to the convexity of the set of decision variables satisfying (21).

It is a well-established result by Prékopa (1995) (Theorem 10.2.1) that this set exhibits convexity under the condition that the law of α constitutes a log-concave probability measure on $\mathbb{R}^{T+\kappa}$. This finding aligns with Prékopa's theorem, which asserts that the law of α is log-concave whenever α possesses a log-concave density, as is the case for the multivariate normal distribution. Leveraging the insights from our residual analysis and the combination of these theorems, we are able to confirm the convex nature of our joint chance constraint problem.

Expectation of the costs for instantaneous grid exchange

We shall assume in this paper that the cost function for instantaneous grid exchange has the concrete form:

$$c_{\gamma,t}(x) = \begin{cases} c_\gamma^* x, & \text{for } x \geq 0, \quad (c_\gamma^* > 0 \text{ given}) \\ 0, & \text{else.} \end{cases}$$

This means that costs for importing unsatisfied energy grow linearly with the amount, whereas excess energy can be get rid off at no costs. Based on this definition of the cost function, we derive in the following how to analytically determine the term $\mathbb{E}[c_{\gamma,t}(\gamma_t(z, \xi, \delta))]$, as required for the objective function (1).

Let $\mu_t = \mu_t(z, \xi, \delta)$ and $\sigma_t^2 = \sigma_t^2(z, \xi, \delta)$ be the expected value and the variance of the random variable γ_t, respectively. Using (2) and the characteristics of the forecasting errors ξ

and δ presented in (18), we derive that

$$\begin{aligned} \mu_t &= d_t - s_t - \Lambda_t - b_t^- + b_t^+ - g_t^+ + g_t^-, \qquad \forall t = 1, \ldots, T+\kappa. \\ \sigma_t^2 &= \sigma_{\xi,t}^2 + \sigma_{\delta,t}^2, \qquad \forall t = 1, \ldots, T+\kappa. \end{aligned} \tag{19}$$

Applying the proof presented in Appendix A, where we denote by $\varphi(\cdot)$ and $\Phi(\cdot)$ the density and distribution function of the standard normal distribution, respectively, we have the function:

$$\mathbb{E}[c_{\gamma,t}(\gamma_t(z,\xi,\delta))] = c_\gamma^* \sigma_t \varphi\left(\frac{\mu_t}{\sigma_t}\right) + c_\gamma^* \mu_t \Phi\left(\frac{\mu_t}{\sigma_t}\right),$$

and, with (19), its gradient with respect to z:

$$\nabla \mathbb{E}[c_{\gamma,t}(\gamma_t(z,\xi,\delta))] = c_\gamma^* \, \Phi\left(\frac{\mu_t}{\sigma_t}\right) \nabla \mu_t \; = \; c_\gamma^* \, \Phi\left(\frac{\mu_t}{\sigma_t}\right) (-e_t, -e_t, \, e_t, \, e_t, -e_t),$$

where e_t denotes the t-th unit vector of dimension $T+\kappa$.

3.4 Probabilistic and expected-value constraints for considering outages

In this section, we present different constraints on reserves for Diesel and battery in the case of weakly-connected mini-grids affected by occasional outages of the main grid. The presentation is top-down according to the quality of the models. We start with a model for joint chance constraints, which is at the core of this paper.

Joint chance constraints (JCC)

As explained before, in the case of a weakly connected mini-grid we expect an outage of the main grid at any initial time τ with a given duration κ. The aim of the dispatch in such case is to retain reserves for Diesel and battery in addition to their regular employment such that the mini-grid can survive in an islanded mode without exchange with the main grid. Since all operational decisions are taken prior to observing uncertainty, successful islanding cannot be guaranteed deterministically but only with a given (possibly high) probability. Satisfying at some fixed time t the true demand $d_t + \delta_t$ (as opposed to the forecasted demand d_t) under the true solar power $s_t + \xi_t$ with the help of scheduled local dispatches of Diesel and battery and additional employment of reserves retained for Diesel and battery, but without having access to the main grid, amounts to the inequality

$$s_t + \xi_t + \Lambda_t + b_t^- - b_t^+ + r_t^b + r_t^\Lambda \geq d_t + \delta_t.$$

Note that we cannot formulate an equality for the load balance here because of the present randomness of some of the parameters which is revealed only after taking the dispatch decisions. The inequality can be reformulated to the following equivalent:

$$\delta_t - \xi_t + d_t - s_t - \Lambda_t - b_t^- + b_t^+ \leq r_t^b + r_t^\Lambda. \tag{20}$$

As mentioned above, we want to satisfy with some high probability p this inequality throughout the time window of an outage starting at time τ and ending at time $\tau + \kappa$. Since the initial time is supposed to be unknown, we formulate a corresponding probabilistic constraint for each τ. Altogether, we obtain the following system of constraints:

$\forall \tau \in \{1, ..., T\}$:

$$\mathbb{P}(\delta_t - \xi_t + d_t - s_t - \Lambda_t - b_t^- + b_t^+ \leq r_t^b + r_t^\Lambda \quad \forall t \in \{\tau, ..., \tau + \kappa\}) \geq p. \tag{21}$$

Each single of these constraints is called a *joint probabilistic constraint* because it involves a system (not just one) of random constraints inside in order to guarantee successful islanding uniformly for the whole time window of an outage. As a consequence, one deals with probabilities under multivariate (not just univariate) normal distributions. This is a particular challenge because no explicit formulae for probabilities are available in this case. Moreover, apart from simply approximating the probabilities themselves (which could be done by some Monte Carlo or Quasi-Monte Carlo sampling), the efficient numerical solution of the arising optimization problems based on solvers from nonlinear programming requires sensitivities of these probabilities with respect to decision variables. Efficiently implementable gradient formulae in the case of Gaussian or related distributions are presented in the form of spherical integrals (e.g., Van Ackooij and Henrion, 2014).

At this point, one might wonder why the joint character of the chance constraints imposed on successful islanding at time index t is not extended to the initial time τ of a potential outage. This would involve placing the quantifier $\forall\tau$ inside rather than outside the probability (21), as seen in hybrid robust-chance-constrained models with infinite (continuously indexed) random inequalities (e.g., González Grandón et al., 2017; van Ackooij et al., 2016). The reason is that during an outage, demand violations can occur multiple times, whereas we assume that the outage itself occurs at most once a day. For instance, if an outage lasts 5 hours, no new outage can start during that period. This motivates us to formulate an individual system with respect to the unknown initial time τ realizing itself at most once. In contrast, individual chance constraints for successful islanding contradict the goal of ensuring robust demand satisfaction throughout the entire outage period. This simplifying but less appropriate model will be discussed for the sake of comparison in the next section.

Individual chance constraints (ICC)

To contrast the JCC model with other more common implementations found in the literature, we introduce in the following the Individual-Chance-Constraints (ICC), which drastically reduces the computational effort but can only ensure the p-level reliability for single time steps and not for the whole outage duration κ.

More precisely, we replace the introduced joint chance constraint system by the following individual chance constraint system:

$$\mathbb{P}(\delta_t - \xi_t + d_t - s_t - \Lambda_t - b_t^- + b_t^+ \leq r_t^{b^-} + r_t^\Lambda) \geq p, \qquad \forall t = 1, \ldots, T + \kappa. \tag{22}$$

Observe that, in contrast with (21), the probability of successful islanding is considered individually for each time step but no longer uniformly over the time window of an outage. As a consequence, the obtained probability function is univariate normal and can be easily inverted using its p-quantile q_p:

$$r_t^{b^-} + r_t^\Lambda - d_t + s_t + \Lambda_t + b_t^- - b_t^+ \geq q_p, \qquad \forall t = 1, \ldots, T + \kappa. \tag{23}$$

In this way, the system (21) of nonlinear, non-explicit and potentially difficult to handle joint chance constraints is reduced to a simple system of explicit linear constraints in the decision variables which is easy to handle numerically. The drawbacks of this model will be illustrated in the numerical results below.

Expected-value constraints ignoring forecasting errors

Next, we further simplify the model by maintaining the assumption of a weakly-connected mini-grid, while completely avoiding probabilistic constraints. Instead, we require that the constraints for successful islanding hold on average. Specifically, this *expected-value dispatch model* does consider outages but only considers the expected value of forecast errors for both solar production and for demand in (20). As a result, the system of constraints describing successful islanding is given by:

$$d_t - s_t - \Lambda_t - b_t^- + b_t^+ \leq r_t^b + r_t^\Lambda, \qquad \forall t = 1, \ldots, T + \kappa. \tag{24}$$

Observe that (24) represents the same linear inequality system as (23) but with different right-hand side.

We note here that we choose to define the system of constraints (23) and (24) for t = $1, \ldots, T + \kappa$ so that we can apply the objective function defined in (3) across all models that consider outages, thus allowing for a comparability between the results of the simplified models (ICC and expected-value models) and the JCC model.

Regular dispatch ignoring outages and forecasting errors

The final model we introduce is the simplest and most basic, as it ignores both forecasting errors and the occurrence of outages from the main-grid. We refer to this as the *regular model* due to its widespread use in the literature, where the operation or economic dispatch of mini-grids often overlooks uncertainties (Beath et al., 2023; Elegeonye et al., 2023; González Grandón et al., 2021; Kumar, 2021; Kumar and Pahuja, 2021). These models typically adopt a deterministic approach, focusing solely on the expected value of the forecasting time series, disregarding both their random errors and the uncertainty of timing of blackouts. The first simplification in this model is the elimination of the last term in the objective function f_0 presented in (3), which accounts for the random instantaneous exchange with the grid. The second simplification concerns the assumption of a strongly connected mini-grid, where outages are disregarded. Consequently, the reserve variables for Diesel and battery systems, which are included in other models to ensure the reliability of supply during blackouts, are also excluded from this model.

Under these simplifications, we obtain the following minimization objective function:

$$f_2(\Lambda, b^+, b^-, g^+, g^-) = \sum_{t=1}^{T+\kappa} \left(c_{\Lambda,t} \cdot \Lambda_t + c_{b,t} \cdot (b_t^+ + b_t^-) - p_{d,t} \cdot d_t + c_{g,t} g_t^+ - p_{g,t} g_t^- \right). \tag{25}$$

We also adjust the power balancing constraint from (9) as follows:

$$s_t + \Lambda_t + b_t^- - b_t^+ + g_t^+ - g_t^-, = d_t \quad \forall t = 1, \ldots, T + \kappa. \tag{26}$$

Furthermore, since the regular model doesn't include any reserve considerations, we adjust the box deterministic constraints for the Diesel and battery discharge variables as shown in (27)-(28), and remove the constraint for the potential state of charge presented in (13). Meanwhile, the constraints (7), (8) and (10)-(12) remain unchanged.

Capacity constraints of the Diesel genset

$$0 \leq \Lambda_t \leq \Lambda^{max}, \qquad \forall t = 1, \ldots, T + \kappa. \tag{27}$$

Capacity constraints of the battery discharge

$$0 \leq b_t^- \leq b^{max}, \qquad \forall t = 1, \ldots, T + \kappa. \tag{28}$$

4 Case study

Our case study focuses on an operational mini-grid in Chifule, an island of Lake Victoria, Tanzania. Currently, the MG remains isolated, lacking any linkage to the main-grid. However, considering the research question at hand and anticipating a future where many MGs in sub-Saharan Africa will be connected to weakly-connected main grids, we assume that the MG, for the purposes of this study, is connected to a main grid characterized by unreliability and frequent outages.

In the following, we present the physical and monetary parameters preset for this case study. For the **random parameters** used in this case study, we refer to Sect. 3.3 where we derive the parameters characterizing the random components of our model, i.e., the mean and (co)-variances of the distribution functions resulting from the presented forecasting models.

Physical parameters

The physical parameters pertinent to this context are detailed in Table 2, while the price and cost parameters are presented in Table 3. In conjunction with the parameters listed in these tables, it is assumed that the nominal time horizon is 24 h, and the time step is set at one hour.

All parameters, excluding those pertaining to the main grid connection, are defined based on data from the MG operator in Tanzania. For the parameters related to the grid connection, we use heuristic and model-informed values. For instance, for the maximum available grid capacity g^{max}, we assume a high value meaning that in case of grid availability, the grid can always guarantee the satisfaction of the local electricity demand. For the average duration of an outage κ, we initially set its value to 3 h, based on empirical values collected from main-grids in similar geographies (Klugman et al., 2021). The κ parameter will be varied, further on, to examine its effect on the obtained solutions. For the probability of an outage ω, we assume that outages occur on nine days out of ten, i.e., $\omega = 0.9$ to magnify the effect of outages on the daily planning of the dispatch.

Monetary parameters

The monetary parameters, presented in Table 3 are also based on indications by the MG operator for the marginal costs of the fuel, the electricity sale price to local customers, and scalar aging costs. The marginal aging cost of the battery is the monetary value reflecting the cost of battery aging due to an additional power unit charged or discharged from the battery Xu et al. (2018). For the cost of importing from the grid and the price of exporting to it, we use values derived from expert interviews with weakly-connected MGs in sub-Saharan Africa. Thereby, we assume that prices and costs differ between night and day, reflecting market conditions, i.e., that importing from the grid costs more during the night than during the day, since at night, the main grid is overall more stressed due to the absence of (cheap) renewable-energy generation (e.g., solar), and that selling to the grid during the day is more valuable due to the higher demand.

Table 2 Physical parameters

	Parameter	Unit	Value	Description
Battery system	η^+	%	95	Average battery charging efficiency
	η^-	%	95	Average battery discharging Efficiency
	σ	%	0	Battery self-discharge rate
	b^{max}	kW	10	Maximal battery charging/dis-Charging rate
	b_{cap}	kWh	100	Maximal battery capacity
	SOC^{max}	%	90	Maximal battery state of charge
	SOC^{min}	%	20	Minimal battery state of charge
	$SOC(t=0)$	%	35	Initial battery state of charge
Diesel genset	Λ^{max}	kW	5	Rated Diesel genset capacity
Main grid connection	g^{max}	kW	100	Maximum available grid capacity
	κ	-	3	Average duration of outages
	ω	-	0.9	Probability of an outage occurring during one day
Solar input	s_t	kW	see Fig. 3	Forecasting of maximum solar Production
Meta-parameters	p	%	90	Probability of Successful islanding
	d_t	kW	see Fig. 2	Forecasted electricity load

Table 3 Cost & price parameters

Parameter	Unit	Values	Description
$c_{\Lambda,t}$	€ /kWh	0.35	Marginal cost of Diesel
$c_{b,t}$	€/kWh	0.0055	Marginal cost of battery
$c_{g,t}$	€/kWh	0.55 (night), 0.15 (day)	Marginal cost of grid import
$c_{\gamma,t}$	€/kWh	0.85 (night), 0.45 (day)	Cost for instantaneous grid exchange
$p_{g,t}$	€/kWh	0.08 (night), 0.13 (day)	Price for grid export
$p_{d,t}$	€/kWh	0.55	Price for electricity sales to customers

5 Results

In this section, we present the results of the optimization problem of the regular (purely-deterministic), expected, ICC and JCC models and compare them to investigate the effects achieved due to the different formulations and ways of handling the uncertainties. For these results, we use the previously presented input parameters and time series.

Optimal dispatch

First, we look into figures 4-7 showcasing the optimal dispatch of each component (respectively-colored bars), in order to meet the *forecasted* electricity demand profile (as

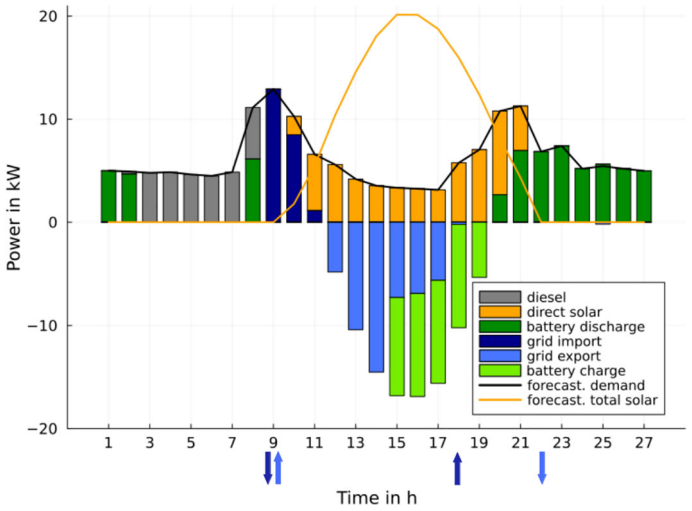

Fig. 4 Economic dispatch in the regular model. Arrows near the x-axis show an increase or a decrease in the price/cost of grid export/import

a continuous black line) given the *forecasted* solar power production (as a continuous yellow line).

To emphasize the price signaling that is implied by the chosen monetary parameters for grid exchange (see Table 3), we show using top and down arrows near the x-axis of the figures the changes in grid import cost (dark blue) and grid export price (light blue). A top arrow indicates an increase in the cost parameter, while a down arrow indicates a decrease. In this sense, the cost of grid import drops to its set lower level at 9 a.m. and increases again to its set higher level at 6 p.m. each day, while the price for grid export increases at 9 a.m. and drops at 10 p.m.

The dispatch of the regular model is shown in Fig. 4. The figure shows that the demand is mainly met through discharging the battery for the first two morning hours and from 10 p.m. to midnight. In the early morning hours starting from 3 a.m., we notice an employment of the Diesel genset. Later, starting from 9 a.m., as the prices for main grid electricity import get cheaper (see Table 3), electricity is also imported from the main grid for a few hours. During the day, the demand is met by using the solar PV generation with a peak around 3 p.m. The solar PV power is first used to meet the electricity demand directly. Any remaining generation from the solar system is either sold to the main grid for additional revenue generation or used to charge the battery in preparation for the night hours. This optimal dispatch leads to expected profits of 84.46 € for the optimization horizon $T + \kappa$, i.e., 27 h.

Looking into the expected-value model, where the model ignores forecasting errors but factor in the possibility of main grid outages occurring with a certain probability, the resulting dispatch shown in Fig. 5 differs from the regular model dispatch, mainly by using the Diesel genset more strongly (throughout the first eight hours of the day) and using more of the excess solar PV generation to charge the battery in the middle of the day. Since the increased Diesel employment adds to the operational costs and the decreased exporting to the main grid reduces the generated profits, the overall expected profits drops to 69.06 € for the optimization horizon of 27 h.

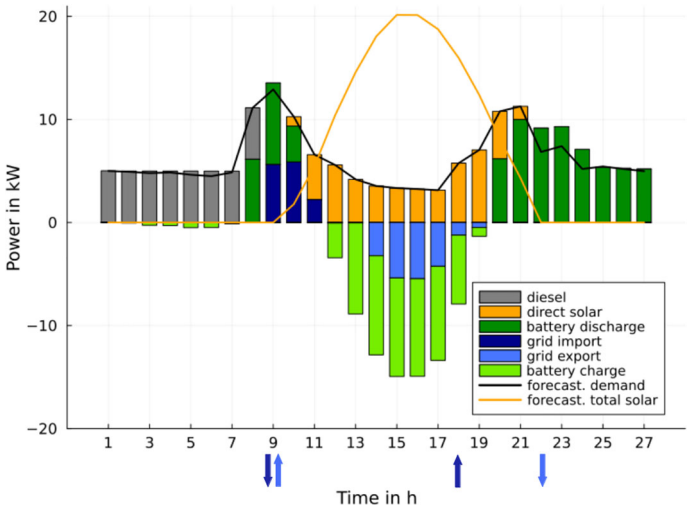

Fig. 5 Economic dispatch for the expected-value model. Arrows near the x-axis show an increase or a decrease in the price/cost of grid export/import

The expected optimal profits drop even more for the ICC model, where we use individual probabilistic constraints to ensure a certain probability of successful islanding while considering both main grid outages and forecasting errors. For a probability of 90%, the optimal profits are 63.73 €. In the resulting optimal dispatch shown in Fig. 6, the optimizer hedges against forecasting errors and main grid outages by starting to charge the battery sooner (i.e., at 1, 2, 5 and 6 a.m.) with electricity imported from the main grid. Additionally, more of the excess electricity is used to charge the battery than to export to the main grid and more Diesel generation occurs during the night hours in order to reduce the electricity discharged from the battery keeping it as a reserve. This new dispatch clearly leads to higher Diesel and main grid import costs and lower main grid export revenues. Overall, compared to the expected-value model, the profits with the ICC model drop by merely 5 €, all while ensuring a high probability in the order of 90% individually at each time step to successfully meet the local demand in an islanded mode and compensate for forecasting errors.

Still, as explained in earlier sections, the ICC model guarantees the required level of islanding probability only for the single time step when an outage starts and doesn't cover the entire duration of the outage. For this, we look into the dispatch results of the JCC model, shown in Fig. 7. The figure showcases the same effects as for the ICC model, only larger in scale, i.e., the dispatch shows more battery charging through main grid imports during the night and excess solar PV power during the day, as well as less battery discharging during the night hours replaced by Diesel generation.

As a consequence, the expected profits drop to 59.87 €, yet with a guarantee that the minigrid survives islanding and probable forecasting errors with a probability of $p = 90\%$ for the whole duration $\kappa = 3$ of the main grid outage. Further in this section, we analyze the influence of the parameters p and κ on the expected profits and achievable successful islanding probabilities.

One concluding remark regarding the optimal dispatch shown in the figures above, is that, except for the regular model which doesn't include any random variables, the planned dispatch from the MG components do not balance out to the *forecasted* demand given the

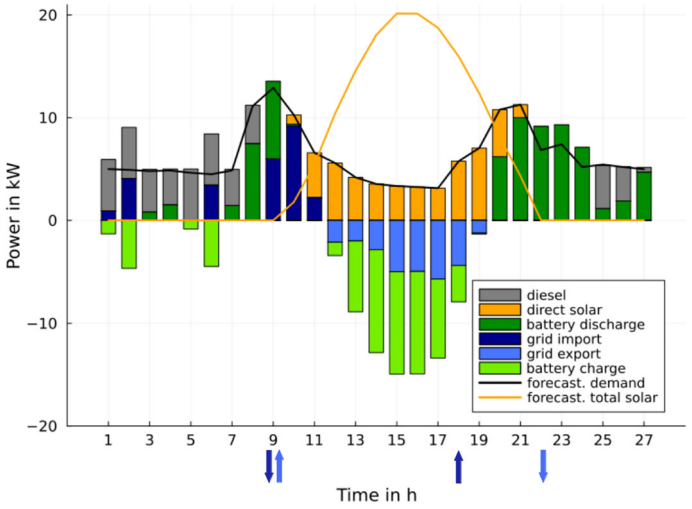

Fig. 6 Economic dispatch for the ICC model. Arrows near the x-axis show an increase or a decrease in the price/cost of grid export/import

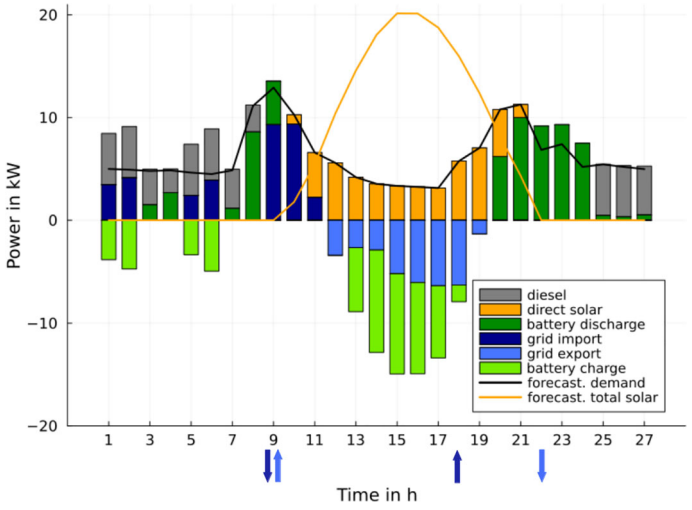

Fig. 7 Economic dispatch for the JCC model. Arrows near the x-axis show an increase or a decrease in the price/cost of grid export/import

forecasted solar power generation. This can be explained by the definition of the balancing constraint as shown in (9). With this equation, we don't impose the expensive condition that *forecasted* demand be met with the respective dispatch from the MG components. Instead, we use for the power balance the *real* demand and the *real* solar power generation, as well as the variable γ_t as a random variable to cover the instantaneous grid exchange (see (2) and the linked explanation in that section of the paper). To showcase this effect in a clearer way, we present, in Fig. 8, the net planned dispatch from all the components in the JCC model in each time step, the forecasted demand and one realization of the real demand. In addition, we showcase the instantaneous dispatch, composed by one realization of the solar power

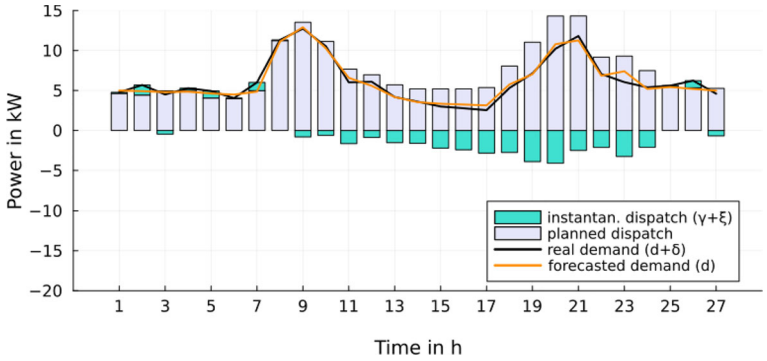

Fig. 8 Planned and instantaneous dispatch of MG components, and forecasted and real demand in the JCC model with $c_{\gamma,t}$ = 0.85 €/kWh (night) and 0.45 €/kWh (day)

forecasting error ξ and the random grid exchange γ. The figure shows clearly the deviations between the planned dispatch and the *forecasted* demand, which are balanced out with the instantaneous dispatch, e.g, at time steps 5 and 7 as a negative deviation from the forecasted demand translating into an instantaneous need for more grid import, and in most other time steps, e.g., at times 9 to 24 as a positive deviation, translating into an instantaneous need for more grid export or generation curtailment.

An immediate result of this modeling logic is that the amount of power that is balanced out using the instantaneous grid component γ_t varies depending on the predetermined cost of γ_t, denoted as $c_{\gamma,t}$: when the the cost associated to the instantaneous grid exchange $c_{\gamma,t}$ and modeled in the objective function using $\mathbb{E}[c_{\gamma,t}(\gamma_t)]$ is higher, less power is balanced using the expensive, instantaneous grid exchange γ and the planned dispatch matches the forecasted demand more. In Appendix B, we showcase the effect of varying $c_{\gamma,t}$ on the resulting dispatch.

Optimal battery cycle

The presented differences in dispatch can also be examined in terms of optimal battery cycling strategy, shown in Fig. 9-12 as charging and discharging powers (in different shades of green) and SOC development (as a continuous black line).

Compared to the cases of the regular and expected-value models, the chance constraint models showcase a strategy to charge the battery overnight, which is understandably more significant in the case of the JCC model. Consistently, the chance constraints models showcase less discharging of the battery in the night hours, this being at the lowest for the JCC model. Looking closer at the range of battery cycling, we note that for the regular and the expected-value model, the state of charge is, as expected, cycled to lower levels than for the ICC and JCC models. In the former two, the state of charge reaches its preset minimum value of 20 %, while, for the ICC, it only goes slightly below 30% and, for the JCC, it remains slightly above 30%.

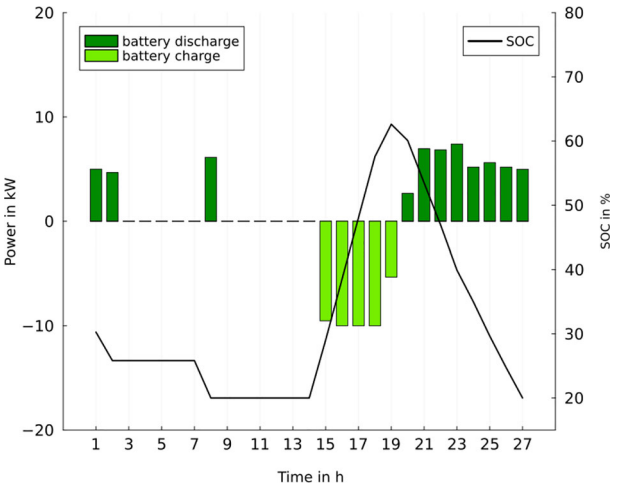

Fig. 9 Battery cycle for the regular model

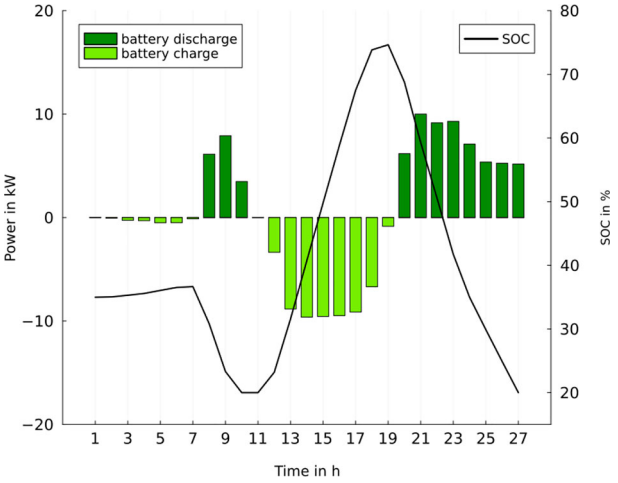

Fig. 10 Battery cycle for the expected-value model

Optimal reserves

Finally, we take a look at the reserves planned for the entire optimization horizon. Starting with the reserves in the case of the expected-value model shown in Fig. 13, we note that the planned diesel reserves cover almost entirely the planned grid import (see Fig 5), thus ensuring that the minigrid succeeds in its islanding provided that there is an outage during these hours that would hinder the import of power.

Fig. 14 presents the planned optimal reserves for the case of an ICC model. Again here, we note that the reserves are planned at each time step of planned grid import, as shown in Fig. 6. During the peak of solar generation in the hours 12-19, where excess electricity is recorded, no reserves are planned.

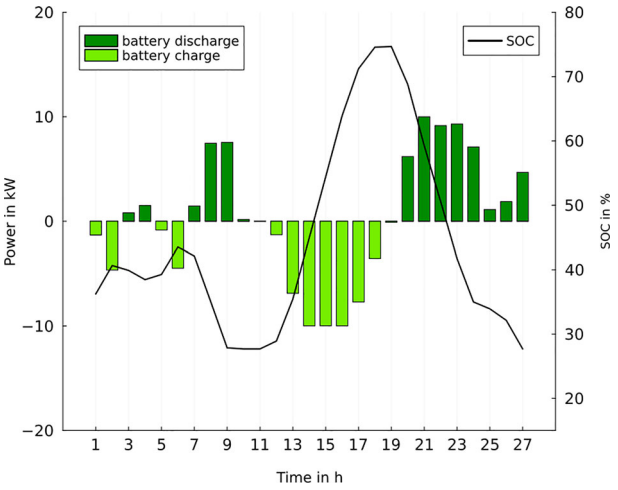

Fig. 11 Battery cycle for the ICC model

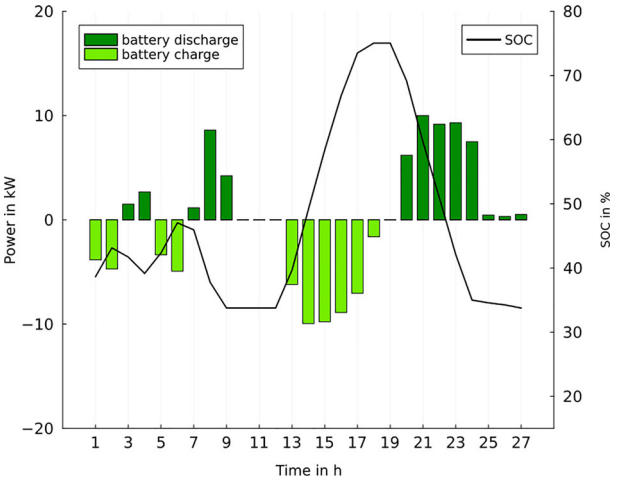

Fig. 12 Battery cycle for the JCC model

For the case of a JCC model, Fig. 15 shows that more battery and Diesel reserves are planned in all time steps and even in more hours of the day than in the ICC case, i.e., only in time steps 13-18, no reserves are present.

The planned reserves translate into additional possible profits that are held back, e.g., through avoided grid export revenues or increased Diesel deployment costs, thus explaining the gradual worsening of the objective function value from the regular to the JCC case (see Table 4). However, in the following, we prove the increased reliability of the MG operation that is achieved by the JCC model, justifying the small drop in profitability showcased so far.

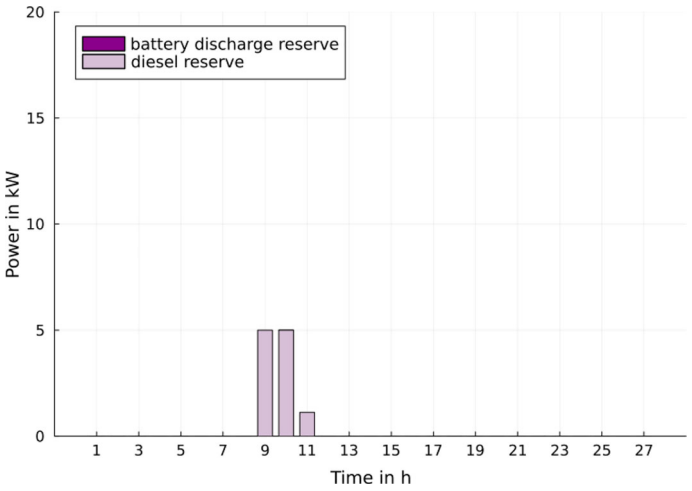

Fig. 13 Reserves for the expected-value dispatch model

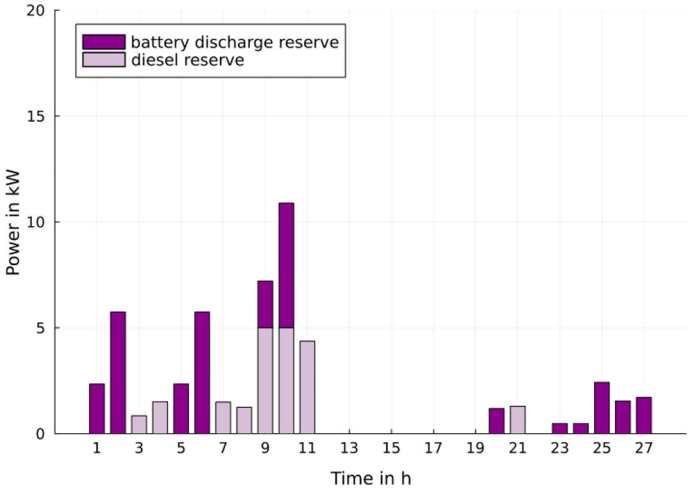

Fig. 14 Reserves for the ICC dispatch model

Increased reliability

With the ICC and JCC model, we are capable of handling many uncertainties in the MG operation, as explained in Sect. 2, thus increasing the reliability of meeting the local electricity demand. Thereby, we handle different types of uncertainty: on the one hand, the uncertainties about the forecasting of the solar PV generation and the electricity demand, on the other hand, the uncertainties about an outage of the main grid. The uncertainties about when and how long a main grid outage could occur enlarges the uncertainties about the forecasting errors: provided that the grid is reliable and doesn't experience any outages during one day, the main grid could level up any forecasting errors and ensure that the power balance is always met. Nevertheless, in the presence of an unreliable grid, not only are forecasting errors

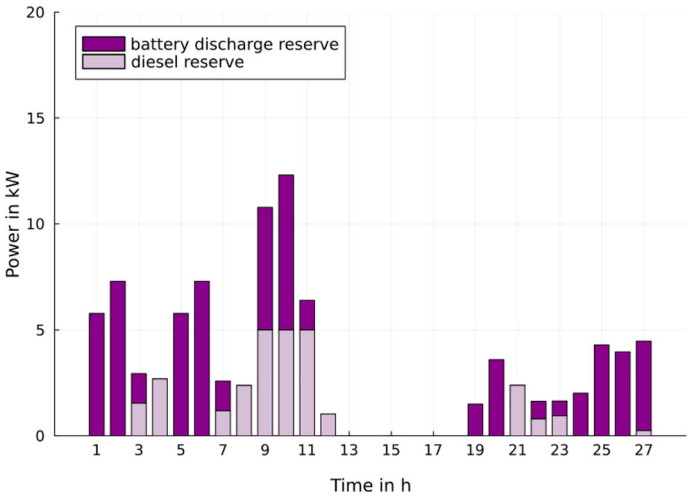

Fig. 15 Reserves for the JCC dispatch model

more noticeable, but any planned grid exchange in the optimal dispatch could also be risky, potentially leading to load shedding and an unmet power balance in the MG.

In the previous figures, we prove that at times of a planned exchange with the main grid, enough reserves from the battery and Diesel are kept in the MG and, therefore, the reliability of meeting the local demand in the case of an outage is increased depending on the preset reliability level (compare Fig. 6 and 7 with Fig. 14 and 15, respectively). In the following figures, we show the effect of the forecasting errors and how the additionally planned reserves can also compensate them even in the case of a main grid outage.

Starting with the ICC case, Fig. 16 showcases, on the left, 10 realizations of the forecasting errors (according to the determined distributions), and on the right, how these errors are compensated using the reserves planned for them. Given that the individual chance constraints are defined as follows and as explained in Sect. 3.4,

$$\mathbb{P}(r_\tau^{b^-} + r_\tau^\Lambda + g_\tau^- - g_\tau^+ - (\xi_\tau + \delta_\tau) \geq 0) \geq p, \qquad \forall \tau \in \{1, ..., 27\},$$

any curves that go below the zero line (colored in red) represent a violation of the probabilistic constraint, and thus, unmet demand translates into lost revenues. Hence, with 10 simulations and a probability $p = 90\%$, an empirical approximate of only one curve in each individual time step should be below zero, hence ensuring that the reliability constraint is satisfied separably for each time step

However, if we look at windows of outages, we find that different lines go below the zero line at different time steps, as represented in Fig. 16 as red-colored lines. Thus, with the ICC model, over the whole duration of the outage, we obtain a probability of successful islanding that is less than 90%. In fact, its empiric value is as low as 58% for the investigated case study for the computed case study(see Table 4). This is precisely the reason behind introducing joint chance constraints which will be discussed next.

In the JCC case, we apply the same logic of verifying the reliability of the MG operation, i.e., the capability of the planned reserves to compensate forecasting errors up to a given probability level. We define the chance constraints as follows (also see Sect. 3):

$$\mathbb{P}(r_t^{b^-} + r_t^\Lambda + g_t^- - g_t^+ - (\xi_t + \delta_t) \geq 0 \ \forall t \in \{\tau, \ldots, \tau + \kappa\}) \geq p, \qquad \forall \tau = 1, ..., 24,$$

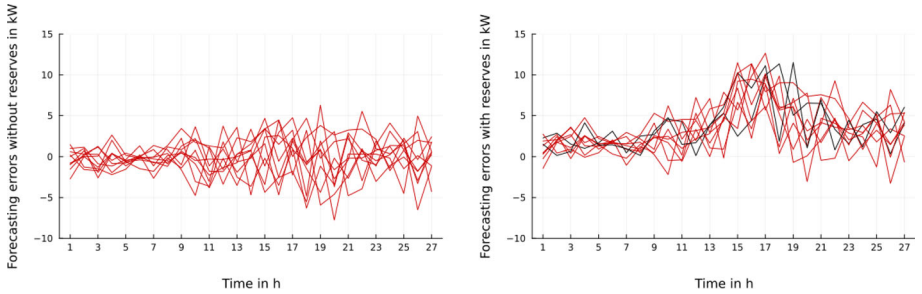

Fig. 16 Forecasting errors of solar PV generation and electricity demand without any planned reserves (left) and with planned reserves (right) in the ICC model

which means that with joint chance constraints, we look into windows of reliability that range between $\tau ... \tau + \kappa$, with $\tau = 1 \dots T$ to verify that the probability level is withheld throughout the entire window, and that, therefore, only one and the same realization curve is below the zero line (colored in red) for each of the windows. This is proven for all possible starting times of an outage $\tau = 1 \dots T$, as shown in Fig. 17 with the outage starting times $\tau = 1, 12, 24$, for example.

Table 4 summarizes some key indicators of solving each of the optimization models, i.e., the optimal profit, the type of model and the required solve time. The values are for an optimization model solved with the input parameters presented in Sect. 4, i.e., a nominal time horizon $T = 24$ and an outage duration $\kappa = 3$ (optimization horizon of 27 steps) and a probability level $p = 90\%$ for ICC and JCC.

Except the regular model, all models are nonlinear. The ICC includes $T + \kappa = 27$ linear chance constraints. The JCC model, on the other hand, includes $T = 24$ nonlinear chance constraints with multivariate probability functions of dimension $\kappa + 1 = 4$. The optimization problem for the expected-value, ICC and JCC models are solved with the local nonlinear solver IPOPT, which is sufficient for global optimality due to the convexity of the defined problems (Prékopa, 1995), and using two methods to compute the probability functions and their gradients: Quasi-Monte-Carlo with the Genz algorithm and Spherical Radial Decomposition (Van Ackooij and Henrion, 2014). Up to a slight numerical imprecision, both computation methods yield the same optimal solution.

Compared to the value of the optimal expected profit of the regular model which is around 84.46 €, the expected-value, ICC and JCC models always lead to less profits, i.e., 69.06 €, 63.73 € and 59.87 € respectively, since they add additional constraints to the feasible set and therefore lead to a worse objective function value. In addition, due to its tighter constraints and the need for increased planning of reserves in order to survive the whole duration of an outage, the JCC model formulation always has a worse objective function value than the expected-value and the ICC. On the other hand, the JCC model achieves a much higher robustness of the minigrid dispatch with regard to main grid outages and forecasting errors. To quantify this increased robustness with a comparable indicator, we calculate, à posteriori to the optimization, the minimally guaranteed probability of successful islanding throughout the entire outage duration for each of the four models by using the joint chance constraint system defined in (21). For the expected-value, ICC and JCC model, we insert the yielded optimal values of the decision variables present in the constraint system. For the regular model, we insert zero values to the reserve decision variables. Table 4 lists the minimally achieved probabilities of successful islanding, denoted as *Min. probability*. As expected,

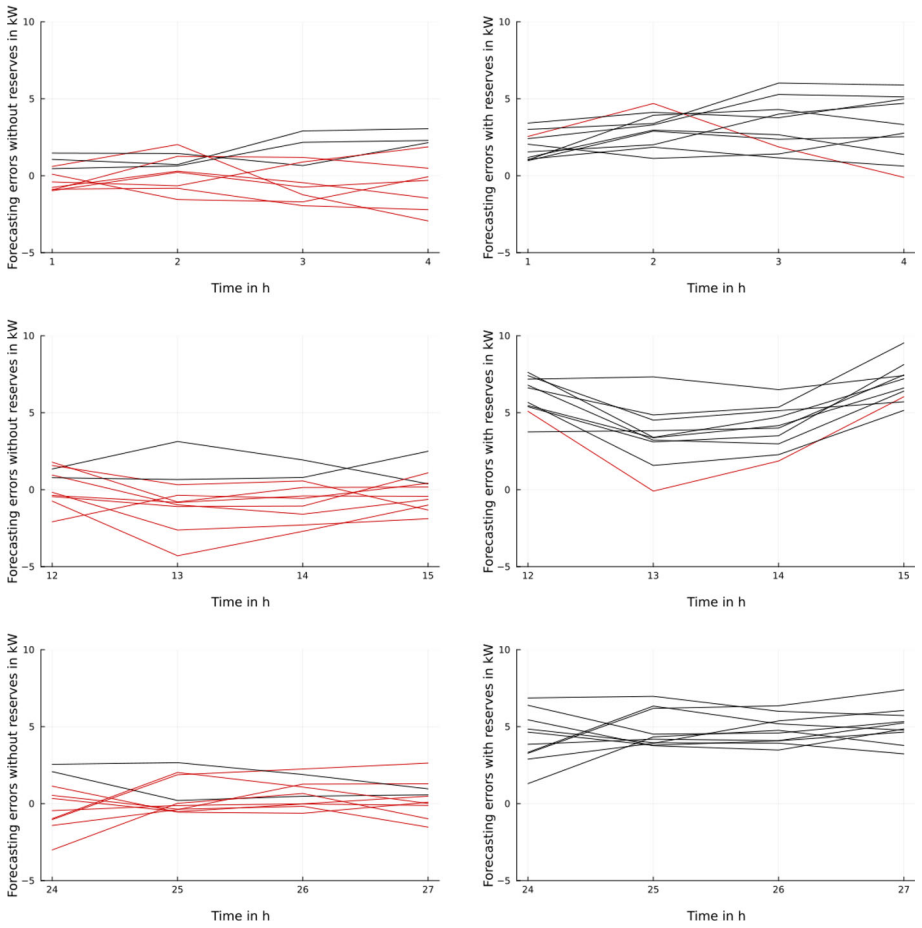

Fig. 17 Forecasting errors of solar PV generation and electricity demand without any planned reserves (left) and with the planned reserves (right) for $\tau = 1$ (top), $\tau = 12$ (middle) and $\tau = 24$ (bottom) in the JCC model with $\kappa = 3$

adding the considerations of reserves and gradually increasing the required level of robustness from merely using expected values, to single step reliability constraints to joint reliability constraints, leads to increasing probabilities of successful islanding with the highest level achieved in the JCC model in the order of 90 % as preset.

In this sense, the drop in profits by approximately 25€ from the regular to JCC model saves the reliability of the minigrid in at least 90% of the cases from certain outages and substantial associated revenue losses, while a mere 9 € loss in profit between the expected-value model and the JCC model guarantees an increase in reliability by 70%.

We note that, in the following table, the indicated solve times are given only as an approximation to hint at the order of magnitude of the required solve times, solely for the given problem setting and its dimensions, as well as the preset accuracy and sample sizes.

Finally, we investigate the effect of changing probability levels p and changing outage duration κ on the optimal results. Figure 18 presents the variation of the optimal expected profits depending on the set probability level. The latter was varied from a value close to 0% up to

Table 4 Comparison of the four models

Modelling approach	Profit	Min. probability	Type	Solve time
Regular	84.46 €	0 %	Linear	< 1 millisecond
Expected-value	69.06 €	20 %	Nonlinear	< 0.5 s
ICC ($p = 90\%$)	63.73 €	58 %	Nonlinear	< 1 s
JCC ($p = 90\%, \kappa = 3$)	59.87 €	90 %	Nonlinear	30-60 s

the maximum probability level above which the problem becomes infeasible. For the present case study, the maximum probability is around 91%. In general, the variation of this parameter, as well as the tendency of the curves depend on the system sizing and the input parameters to the optimization problem. As shown in the figure, the trend is such that higher p-levels lead to a worse objective function value, since this means an increase of the reliability and, therefore, more hedging against the uncertainty leading to an overall decrease in profits.

To investigate the effect of varying κ, we look into the maximal reliability level (referred to hereafter as p-max problem) that is feasible given the sizing of the studied MG as well as the boundary conditions. Formulating the p-max problem requires changing the objective function to a maximization of the probability level p, which is changed from being an input parameter to being a decision variable. Figure 19 presents the maximal reliability level for values of the outage duration κ between one and ten. It shows that the higher the outage duration, the lower is the maximal reliability to be achieved. Already with an outage lasting $\kappa = 5$ hours, the probability of successful islanding drops below 60%, and for $\kappa = 7$ hours, it drops to almost 0%. This means that, with outages lasting 7 h or longer and with the given MG sizing, the maximum reserves that can be planned are not enough to achieve a non-zero probability of successful islanding.

Hence, in order to achieve high probabilities of successful islanding for a higher outage duration, we need to adjust the size of the minigrid and therefore, solve the respective sizing problem, e.g., by combining it with the dispatch optimization problem using chance constraints. Depending on the assumed input parameters, the assumed duration of the outage and the reliability level to be achieved, the solution to this problem could be too expensive and, therefore, must be considered in trade-off with the value of robustness achieved by using chance constraints.

Overall, we prove that, through using joint chance constraints, a level of successful islanding probability can be preset and guaranteed, increasing the robustness of the optimal MG operation strategy under uncertainty, in exchange with a small drop in profitability. This trade-off is quickly compensated for, given the high reliability level that is achieved. Without this level of reliability, experiencing an outage leads to very high costs represented by load shed and, therefore, electricity purchases that are missing.

Practically, when applying dispatch models to the real-time operation of mini-grids, operators implement the dispatch algorithms in a rolling horizon method, typically of 15 min, thus updating the operation at each new run with new input data and forecast values. This method should also be applied when using the presented JCC model, as this increases the practical dispatch's adaptability to new boundary conditions.

Supplementary information. The code with the model implementation and results can be found on the Autarky-Power github page.

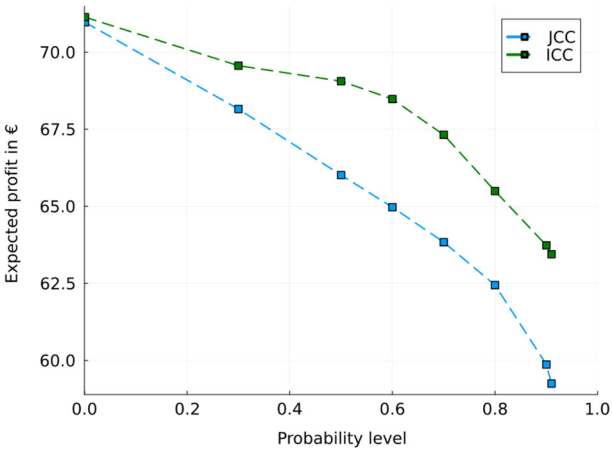

Fig. 18 Variation of the objective function for the ICC (green) and the JCC (blue) model formulation depending on the probability level

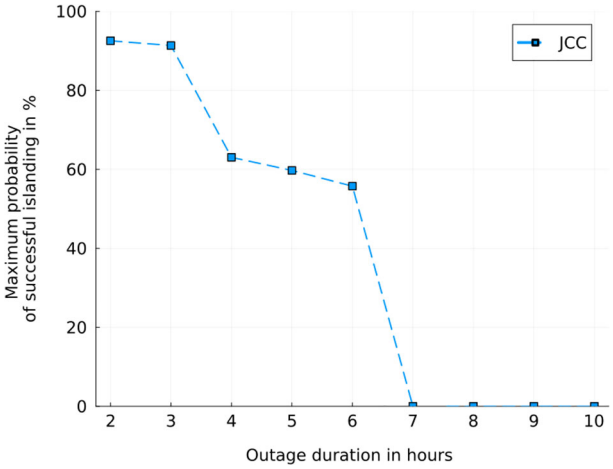

Fig. 19 Variation of the maximum probability of successful islanding of the JCC model formulation depending on the outage duration

Appendix A Expected cost for stochastic grid exchange

Let $\zeta \sim \mathcal{N}(\mu, \sigma^2)$ be a Gaussian Random variable with mean $\mu \in \mathbb{R}$ and standard deviation $\sigma \in \mathbb{R}$. Consider the piecewise linear cost function

$$h(y) = \begin{cases} cy, & \text{if } y \geq 0, \\ 0, & \text{otherwise,} \end{cases} \tag{A1}$$

where $c > 0$ is given.

Expected cost

The expected cost $\mathbb{E}[h(\zeta)]$ with respect to the distribution of ζ is given by

$$\mathbb{E}[h(\zeta)] = \frac{1}{\sigma\sqrt{2\pi}} \int_{-\infty}^{\infty} h(y) e^{-\frac{1}{2\sigma^2}(y-\mu)^2} dy.$$

The substitution $y := \sigma x + \mu$ allows for transformation to standard normal distribution. In particular, having $dy = \sigma dx$, and, by applying (A1), we may continue the above equation as follows:

$$\begin{aligned}
\mathbb{E}[h(\zeta)] &= \frac{1}{\sqrt{2\pi}} \int_{-\infty}^{\infty} h(\sigma x + \mu) e^{-\frac{1}{2}x^2} dx \\
&= \frac{1}{\sqrt{2\pi}} \int_{-\frac{\mu}{\sigma}}^{\infty} c(\sigma x + \mu) e^{-\frac{1}{2}x^2} dx \\
&= \frac{c\sigma}{\sqrt{2\pi}} \int_{-\frac{\mu}{\sigma}}^{\infty} x e^{-\frac{1}{2}x^2} dx + \frac{c\mu}{\sqrt{2\pi}} \int_{-\frac{\mu}{\sigma}}^{\infty} e^{-\frac{1}{2}x^2} dx.
\end{aligned}$$

Denoting by $\varphi(\cdot)$ and $\Phi(\cdot)$ the density and distribution function of the standard normal distribution, respectively, we are able to resolve both integrals and arrive at the equation

$$\mathbb{E}[h(\zeta)] = c\sigma\varphi\left(\frac{\mu}{\sigma}\right) + c\mu\Phi\left(\frac{\mu}{\sigma}\right).$$

Note, we used the property $\varphi'(x) = -x\varphi(x)$ in order to resolve the first integral.

Gradient

Assuming a dependency on an outer parameter (variable) z: In particular, let $\mu = \mu(z)$ and $\sigma = \sigma(z)$ be functions depending on the variable z. Then, also the sensitivity of the expected cost above in terms of the variable z may be of interest. Denoting with $\nabla\mu$ and $\nabla\sigma$ the gradients of μ and σ with respect to z we have

$$\begin{aligned}
\nabla\mathbb{E}[h(\zeta(z))] &= c\varphi\left(\frac{\mu}{\sigma}\right)\nabla\sigma - c\mu\varphi\left(\frac{\mu}{\sigma}\right)\frac{\sigma\nabla\mu - \mu\nabla\sigma}{\sigma^2} \\
&\quad + c\,\Phi\left(\frac{\mu}{\sigma}\right)\nabla\mu + c\mu\varphi\left(\frac{\mu}{\sigma}\right)\frac{\sigma\nabla\mu - \mu\nabla\sigma}{\sigma^2} \\
&= c\varphi\left(\frac{\mu}{\sigma}\right)\nabla\sigma + c\,\Phi\left(\frac{\mu}{\sigma}\right)\nabla\mu.
\end{aligned}$$

Under the assumption that only μ is depending on z in fact ($\nabla\sigma = 0$), then the gradient formula further simplifies just to

$$\nabla\mathbb{E}[h(\zeta(z))] = c\,\Phi\left(\frac{\mu}{\sigma}\right)\nabla\mu.$$

Appendix B Effect of varying the cost parameter associated with the instantaneous grid exchange $c_{\gamma,t}$

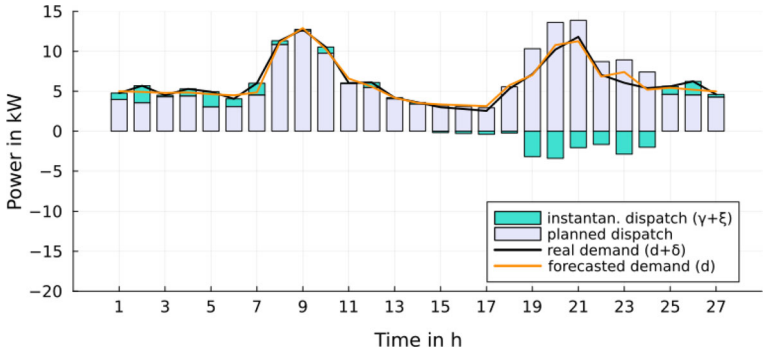

Fig. 20 Planned and instantaneous dispatch of MG components, and forecasted and real demand in the JCC model with $c_{\gamma,t} = 0.65$ €/kWh (night) and 0.25 €/kWh (day)

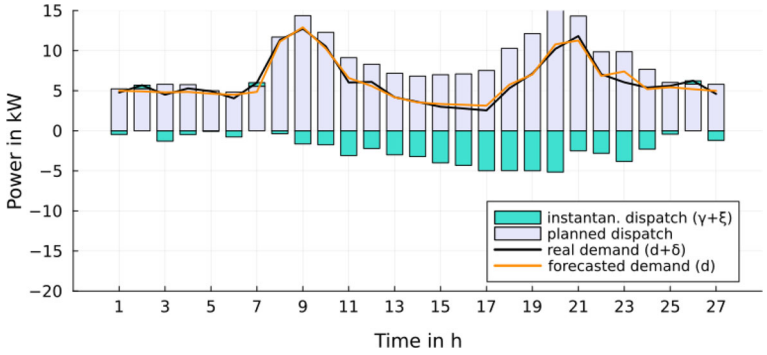

Fig. 21 Planned and instantaneous dispatch of MG components, and forecasted and real demand in the JCC model with $c_{\gamma,t} = 1.35$ €/kWh (night) and 0.95 €/kWh (day)

Acknowledgements We thank INENSUS GmbH for their commitment to open science by sharing real power measurement data from one of their mini-grid subsidiaries in Tanzania. The second author is thankful for the support by the Fondation Mathématique Jacques Hadamard (FMJH) Program Gaspard Monge in optimization and operations research including support to this program by Électricité De France (EDF) No P-2022-0022. The third author is thankful for the support by the Deutsche Forschungsgemeinschaft (DFG) in the Collaborative Research Centre CRC/Transregio 154, Mathematical Modelling, Simulation and Optimization Using the Example of Gas Networks, Project B04. The fourth author acknowledges the support by the DFG ExC 2046 MATH+: Berlin Mathematics Research Center under project AA4-10.

Funding Open Access funding enabled and organized by Projekt DEAL.

Declarations

Conflict of interest The authors declare that they have no known competing financial or non-financial interests that could have appeared to influence the work reported in this paper.

References

Antonanzas-Torres, F., Antonanzas, J., & Blanco-Fernandez, J. (2021). State-of-theart of mini grids for rural electrification in West Africa. *Energies, 14*(4), 990. https://doi.org/10.3390/en14040990

Beath, H., Baranda Alonso, J., Mori, R., Gambhir, A., Nelson, J., & Sandwell, P. (2023). Maximising the benefits of renewable energy infrastructure in displacement settings: Optimising the operation of a solar-hybrid mini-grid for institutional and business users in mahama refugee camp, rwanda. *Renewable and Sustainable Energy Reviews, 176*, 113142. https://doi.org/10.1016/j.rser.2022.113142

Berthold, H., Heitsch, H., Henrion, R., & Schwientek, J. (2022). On the algorithmic solution of optimization problems subject to probabilistic/robust (probust) constraints. *Math. Oper. Res., 96*(1), 1–37. https://doi.org/10.1080/02331934.2019.1576670

Box, G., & Jenkins, G. M. (1976). *Time series analysis: Forecasting and control*. Holden-Day.

Charnes, A., & Cooper, W. W. (1959). Chance-constrained programming. *Management Science, 5*, 73–79. https://doi.org/10.1287/mnsc.6.1.73

Elegeonye, H. I., Owolabi, A. B., Ohunakin, O. S., Yakub, A. O., Yahaya, A., Same, N. N., Suh, D., & Huh, J.-S. (2023). Techno-economic optimization of mini-grid systems in nigeria: A case study of a pv-battery-diesel hybrid system. *Energies, 16*(12), 4645. https://doi.org/10.3390/en16124645

Farshbaf-Shaker, M. H., Gugat, M., Heitsch, H., & Henrion, R. (2020). Optimal Neumann boundary control of a vibrating string with uncertain initial data and probabilistic terminal constraints. *SIAM J. Optim., 58*(4), 2288–2311. https://doi.org/10.1137/19M1269944

González Grandón, T., Heitsch, H., & Henrion, R. (2017). A joint model of probabilistic/robust constraints for gas transport management in stationary networks. *Computational Management Science, 14*(3), 443–460. https://doi.org/10.1007/s10287-017-0284-7

González Grandón, T., Henrion, R., & Pérez-Aros, P. (2022). Dynamic probabilistic constraints under continuous random distributions. *Mathematical Programming, 196*(1), 1065–1096. https://doi.org/10.1007/s10107-020-01593-z

González Grandón, T., Schwenzer, J., Steens, T., & Breuing, J. (2024). Electricity demand forecasting with hybrid classical statistical and machine learning algorithms: Case study of ukraine. *Applied Energy, 355*, 122249. https://doi.org/10.1016/j.apenergy.2023.122249

González Grandón, T., de Cuadra García, F., & Pérez-Arriaga, I. (2021). A market-driven management model for renewable-powered undergrid mini-grids. *Energies, 14*(23), 7881. https://doi.org/10.3390/en14237881

Heitsch, H. (2020). On probabilistic capacity maximization in a stationary gas network. *Optimization, 69*(3), 575–604. https://doi.org/10.1080/02331934.2019.1625353

Hong, Y.-Y., Apolinario, G. F. D., Lu, T.-K., & Chu, C.-C. (2022). Chance-constrained unit commitment with energy storage systems in electric power systems. *Energy Reports, 8*, 1067–1090. https://doi.org/10.1016/j.egyr.2021.12.035

IEA (2020). Tracking SDG7: The energy progress report. Retrieved from https://www.iea.org/reports/tracking-sdg7-the-energy-progress-report-2020

Inensus (2014). Mini-grid policy toolkit. (EU Energy Initiative Partnership Dialogue Facility (EUEI-PDF))

Klugman, N., Adkins, J., Paszkiewicz, E., Hickman, M. G., Podolsky, M., Taneja, J., & Dutta, P. (2021). Watching the grid: Utility-independent measurements of electricity reliability in Accra, Ghana.

Kumar, S. (2021). Cost-based unit commitment in a stand-alone hybrid microgrid with demand response flexibility. *Journal of The Institution of Engineers (India): Series B,103*, 51–61. https://doi.org/10.1007/s40031-021-00634-1

Kumar, S., & Pahuja, G.L. (2021). Optimal power dispatch of renewable energy-based microgrid with AC/DC constraints. O.H. Gupta & V.K. Sood (Eds.), Recent advances in power systems (pp. 59–76). Singapore: Springer Singapore.

Liu, G., Starke, M., Xiao, B., Zhang, X., & Tomsovic, K. (2017). Microgrid optimal scheduling with chance-constrained islanding capability. *Electric Power Systems Research, 145*, 197–206. https://doi.org/10.1016/j.epsr.2017.01.014

Loiaciga, H. (1988). On the use of chance constraints in reservoir design and operation modeling. *Water Resources Management, 24*, 1969–1975. https://doi.org/10.1029/WR024i011p01969

Parisio, A., Rikos, E., & Glielmo, L. (2014). A model predictive control approach to microgrid operation optimization. *IEEE Transactions on Control Systems Technology, 22*(5), 1813–1827. https://doi.org/10.1109/TCST.2013.2295737

Peña-Ordieres, A., Molzahn, D. K., Roald, L. A., & Wächter, A. (2021). DC optimal power flow with joint chance constraints. *IEEE Transactions on Power Systems, 36*(1), 147–158. https://doi.org/10.1109/TPWRS.2020.3004023

Prékopa, A. (1995). *Stochastic programming*. Dordrecht: Kluwer Academic Publishers.

Prékopa, A., & Sántai, T. (1978). Flood control reservoir system design using stochastic programming. In M. L. Balinski & C. Lemarechal (Eds.), *Mathematical programming in use* (pp. 138–151). Berlin: Springer.

R Core Team (2021). R: A language and environment for statistical computing [Computer software manual]. Vienna, Austria. Retrieved from https://www.Rproject.org/

Rocky Mountain Institute (2018). Under the grid: Improving the economics and reliability of rural electricity service with undergrid minigrids [Computer software manual]. Retrieved from https://rmi.org/insight/under.the-grid/

Sen, P., Roy, M., & Pal, P. (2016). Application of arima for forecasting energy consumption and ghg emission: A case study of an indian pig iron manufacturing organization. *Energy, 116*, 1031–1038. https://doi.org/10.1016/j.energy.2016.10.068

Shapiro, A., Dentcheva, D., & Ruszczyński, A. (2014). *Lectures on stochastic programming: Modeling and theory* (2nd ed.). Philadelphia: Society for Industrial and Applied Mathematics.

van Ackooij, W., Frangioni, A., & de Oliveira, W. (2016). Inexact stabilized benders' decomposition approaches with application to chance-constrained problems with finite support. *Computational Optimization and Applications, 65*(3), 637–669. https://doi.org/10.1007/s10589-016-9851-z. Retrieved from.

Van Ackooij, W., & Henrion, R. (2014). Gradient formulae for nonlinear probabilistic constraints with gaussian and gaussian-like distributions. *SIAM Journal on Optimization, 24*(4), 1864–1889. https://doi.org/10.1137/130922689

Van Ackooij, W., Henrion, R., Möller, A., & Zorgati, R. (2010). On probabilistic constraints induced by rectangular sets and multivariate normal distributions. *Mathematical Methods of Operations Research, 71*(3), 535–549. https://doi.org/10.1007/s00186-010-0316-3

van Ackooij, W., Henrion, R., Möller, A., & Zorgati, R. (2014). Joint chance constrained programming for hydro reservoir management. *Optimization and Engineering, 15*(2), 509–531. https://doi.org/10.1007/s11081-013-9236-4

Xu, B., Zhao, J., Zheng, T., Litvinov, E., & Kirschen, D. S. (2018). Factoring the cycle aging cost of batteries participating in electricity markets. *IEEE Transactions on Power Systems, 33*(2), 2248–2259. https://doi.org/10.1109/TPWRS.2017.2733339

Zhao, B., Shi, Y., Dong, X., Luan, W., & Bornemann, J. (2014). Short-term operation scheduling in renewable-powered microgrids: A duality-based approach. *IEEE Transactions on Sustainable Energy, 5*(1), 209–217. https://doi.org/10.1109/TSTE.2013.2279837